DALTON

Magnetic properties of dinuclear copper(II) complexes with a N_6 pyridazine-derived ligand *

Evgenia Spodine,[a] Ana María Atria,[a] Jorge Manzur,[b] Ana María García,[b] María Teresa Garland,[b] Alexandre Hocquet,[b] Eduardo Sanhueza,[b] Ricardo Baggio,[c] Octavio Peña[d] and Jean-Yves Saillard[d]

[a] *Facultad de Ciencias Químicas y Farmacéuticas, Universidad de Chile, Casilla 233, Santiago, Chile*
[b] *Facultad de Ciencias Físicas y Matemáticas, Universidad de Chile, Casilla 2777, Santiago, Chile*
[c] *Departamento de Física, Comisión de Energía Nuclear, Buenos Aires, Argentina*
[d] *UMR 6511 au CNRS, Université de Rennes I, 35042 Rennes Cedex, France*

A new hexadentate ligand 3,6-bis[(6-methyl-2-pyridyl)(2-pyridyl)methyl]pyridazine (mbdpdz) was prepared by a condensation reaction of 3,6-dichloropyridazine and (6-methyl-2-pyridyl)(2-pyridyl)methyllithium, and the following binuclear copper(II) complexes were obtained: $[Cu_2(mbdpdz)Cl_4]$ **1**, $[Cu_2(mbdpdz)Br_4]$ **2**, $[Cu_2(mbdpdz)Cl_2(OH)]Cl$ **3** and $[Cu_2(mbdpdz)Br_2(OH)]Br$ **4**. The crystal and molecular structures of the two isomorphous complexes **3** and **4** are reported. Both complexes crystallize in the monoclinic system, space group *C*2/*c*, with eight formula units per unit cell. Complex **3**: $a = 28.364(3)$, $b = 13.511(1)$, $c = 16.858(1)$ Å, $\beta = 109.70(1)°$. Complex **4**: $a = 28.528(5)$, $b = 13.459(2)$, $c = 17.348(3)$ Å, $\beta = 109.35(1)°$. The copper centres in the binuclear cation in **3** and **4** have a square-pyramidal geometry, with a bridging hydroxide angle of 115.1(3) and 116.2(5)° respectively. The Cu · · · Cu distance was 3.251(2) Å in both binuclear complexes. These hydroxo-bridged complexes were obtained by refluxing acetonitrile–water suspensions of **1** and **2**, respectively. Variable-temperature magnetic studies on all complexes indicate the existence of antiferromagnetic exchange phenomena. Extended-Hückel calculations were performed on complexes **3** and **4** in order to identify the electronic origin of the spin coupling of these molecules.

Binucleating pyrazolyl, pyridazine and phthalazine ligands form predominantly binuclear copper(II) complexes in which, in many cases, the metal centres are bridged by a hydroxide group in addition to the diazine moiety.

The hydroxo-bridged diazine-bridged compounds studied by Thompson and co-workers[1–11] can be roughly divided into two groups: those involving five-membered chelate rings and those involving six-membered rings. Owing to geometrical restrictions imposed by these chelate rings, the Cu–O–Cu bridge angle falls into two ranges; smaller angles for six-membered rings (100–116°) and larger ones for five-membered rings (116–127°). The antiferromagnetic interactions found are larger for the latter complexes. These studies emphasize the role of the hydroxide bridge as the principal exchange pathway in the hydroxo-bridged complexes.

However, the principal aim of the above mentioned work concerned complexes with N_4 diazine ligands. We herein present the syntheses of binuclear copper(II) complexes with new hexadentate ligands, derived from pyridazine, which present six-membered chelate rings around the metal centres {N_6: 3,6-bis[(6-methyl-2-pyridyl)(2-pyridyl)methyl]pyridazine}.

Results and Discussion

As has been observed with complexes of other pyridazine- and phthalazine-derived ligands, in the syntheses of copper chloride and bromide complexes of 3,6-bis[(6-methyl-2-pyridyl)(2-pyridyl)methyl]pyridazine (mbdpdz), binuclear tetrahalide derivatives are produced when the water content is minimized. However, when water is used as solvent the hydroxide derivatives are obtained.

The structure of the halide derivatives of the mbdpdz ligand, $[Cu_2(mbdpdz)X_4]$ (X = Cl **1** or Br **2**), could not be determined since good single crystals could not be grown from common organic solvents due to the limited solubility of the compounds. Only when the complexes were dissolved in hot water, crystals of the hydroxo derivatives were obtained, and their structures determined by X-ray diffraction.

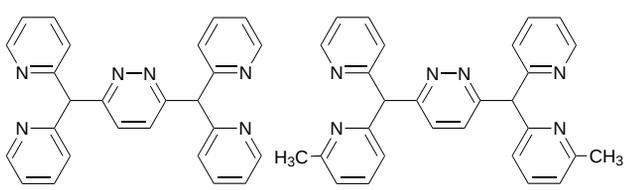

Chloro complex 1 and bromo complex 2

The structure of complex **1** should be quite similar to that shown by $[Cu_2(bdpdz)Cl_3(H_2O)]Cl$ [bdpdz = 3,6-bis(di-2-pyridylmethyl)pyridazine].[12] Therefore, a significantly distorted octahedral geometry at each copper(II) centre can be inferred, with two chloride bridges between the two metal centres together with the bridging diazine ligand. The existence of co-ordinated water in **1**, as in $[Cu_2(bdpdz)Cl_3(H_2O)]Cl$ is not evident due to the facility that exists in the generation of hydroxo species with the mbdpdz ligand. However, the elemental analysis of the complex corresponds to $[Cu_2(mbdpdz)Cl_4]\cdot 2H_2O$.

The assumption of similar structures is based on the almost identical magnetic behaviour that is shown by the two binuclear complexes. The binuclear species **1** shows magnetic coupling between the metal centres. This antiferromagnetic behaviour can be quantified by the calculated J value of -36 cm^{-1}, which compares well with $J = -39.8$ cm^{-1} for $[Cu_2(bdpdz)Cl_3(H_2O)]Cl$. The variable-temperature magnetic susceptibility data for complex **1** are shown in Fig. 1. The best fit was calculated from the modified Bleaney–Bowers equation for exchange-coupled pairs of copper(II) ions,[13] as shown in equation (1). In

* *Non-SI units employed*: $\mu_B \approx 9.274 \times 10^{-24}$ J T^{-1}; eV $\approx 1.602 \times 10^{-19}$ J; cal = 4.184 J; G = 10^{-4} T.

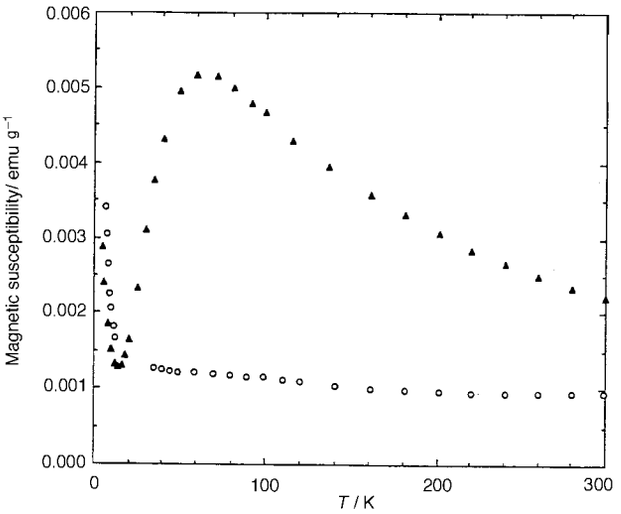

Fig. 1 Corrected magnetic susceptibility *vs.* temperature for (▲) $[Cu_2(mbdpdz)Cl_4]\cdot 2H_2O$ **1** and (○) $[Cu_2(mbdpdz)Cl_2(OH)]Cl$ **3**

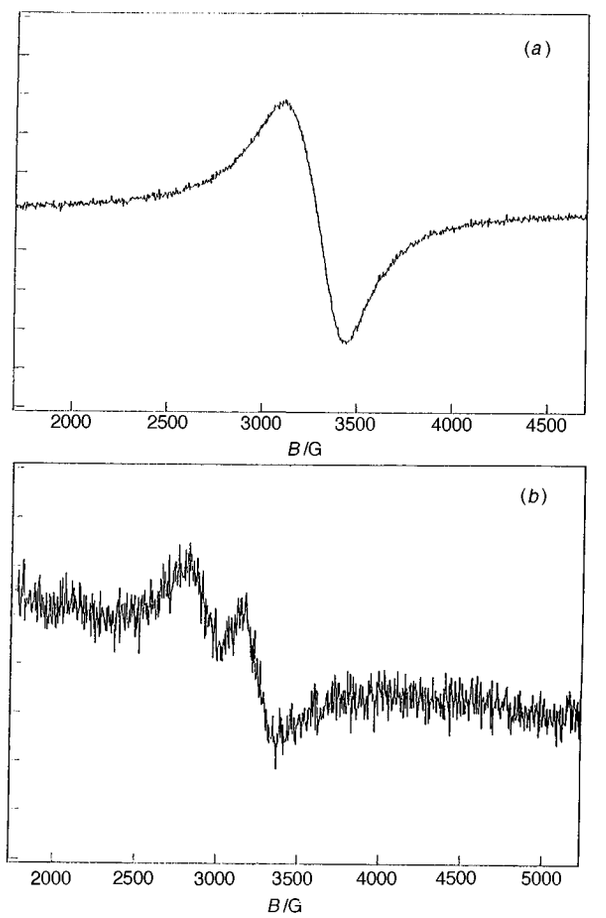

Fig. 2 The EPR spectra of (*a*) $[Cu_2(mbdpdz)Cl_4]\cdot 2H_2O$ **1** and (*b*) $[Cu_2(mbdpdz)Cl_2(OH)]Cl$ **3** at room temperature

$$\chi_M = \frac{N\beta^2 g^2}{3kT}[1 + \tfrac{1}{3}\{\exp(-2J)\}]^{-1}(1-\gamma) + \left[\frac{N\beta^2 g^2}{4kT}\right]\gamma + N\alpha \quad (1)$$

this expression all symbols have their usual meaning. The parameters giving the best fit were obtained by using a non-linear regression analysis. The exchange integral for **1** was $2J = -72$ cm^{-1}, the fraction of magnetically dilute copper(II) impurity $\gamma = 0.04$ and $g = 1.91$; $N\alpha$ was taken as 120 cm^3 mol^{-1}.

The low value obtained for g can be attributed to inter-

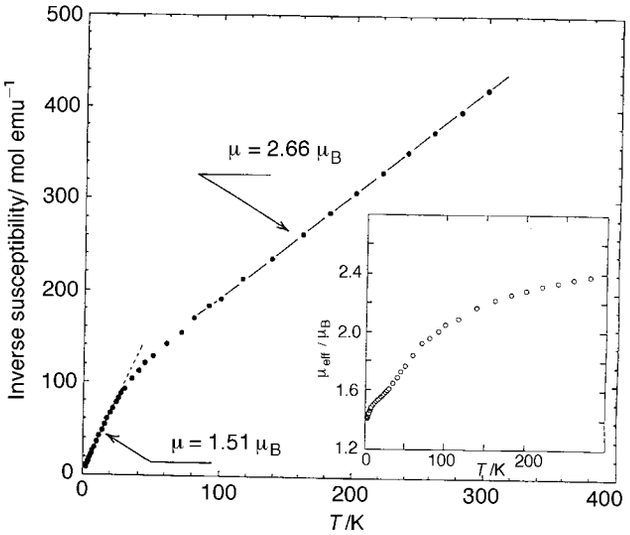

Fig. 3 Inverse corrected magnetic susceptibility *vs.* temperature for $[Cu_2(mbdpdz)Br_4]\cdot H_2O$ **2**

molecular spin coupling interactions, thus indicating that the simple Bleaney–Bowers equation is not the best mathematical expression to fit the experimental susceptibility data. Thus the polycrystalline room-temperature powder EPR spectrum of complex **1** consists of a single, quasi-symmetrical signal, with no hyperfine splitting and no signal at half-field, which allows the calculation of $g = 2.12$ (Fig. 2).

For the bromo complex **2**, elemental analysis indicates that a binuclear species is also formed, as in the case of chloro complex **1**. Magnetic measurements made on $[Cu_2(mbdpdz)Br_4]\cdot H_2O$ show strong temperature dependence of magnetic moment per dimer, dropping from a value of 2.66 μ_B at 300 K to 1.51 μ_B at 5 K (Fig. 3). The plot of the inverse susceptibility *versus* temperature shows two distinct linear dependence ranges. If one calculates the effective magnetic moment from the χT product for each temperature, a monotonic decrease is observed from room temperature to 2 K (insert Fig. 3). This behaviour can only be explained by supposing that intermolecular interactions become important as the temperature is lowered. The powder EPR spectrum of **2** at room temperature is similar to the one recorded for **1**, and allows the calculation of a g value of 2.12.

$[Cu_2(mbdpdz)Cl_2(OH)]Cl$ 3 and $[Cu_2(mbdpdz)Br_2(OH)]Br$ 4

Binuclear complexes **3** and **4** are isostructural with very similar geometry and dimensions involving the hexadentate ligand and the two copper(II) centres. The binuclear unit is bridged by the organic molecule and by the hydroxide group. Both complexes present one terminal halogen atom in the first co-ordination sphere of each metal. Complexes **3** and **4** are stabilized by an external, non-co-ordinated halogen ion, the latter being severely disordered.

The structure of **3** and **4** is shown in Fig. 4, and interatomic distances and angles relevant to the copper co-ordination spheres are given in Tables 1 and 2. The binuclear cationic complex is not flat, with the two copper(II) atoms bound to four in-plane (N_2OCl) donors with Cu–N and Cu–O distances close to 2.0 Å, and Cu–Cl distances of 2.255(3) and 2.252(3) Å, and Cu–Br distances of 2.392(2) and 2.405(2) Å, respectively. The apical Cu(1)–N(3) and Cu(2)–N(6) distances are 2.264(6) and 2.321(7) for **3**, and 2.261(9) and 2.334(9) for **4**. For complex **3** the deviations of the atoms from the best mean plane defined for the Cu(1)–O(1)–Cu(2)–N(4)–N(1) ring are −0.008, 0.84, 0.008, −0.018 and 0.018 Å. Similar values are found for the complex **4** Cu(1)–O(1)–Cu(2)–N(4)–N(1) ring (−0.006, 0.83, 0.006, −0.015, 0.015 Å).

The stereochemistry at each metal atom is square pyramidal.

Table 1 Selected interatomic distances (Å) and angles (°) for complex **3**

Cu(1)–O(1)	1.930(7)	Cu(1)–N(2)	2.015(7)
Cu(1)–N(1)	2.043(6)	Cu(1)–Cl(1)	2.252(3)
Cu(1)–N(3)	2.264(6)	Cu(2)–O(1)	1.921(6)
Cu(2)–N(5)	2.021(6)	Cu(2)–N(4)	2.057(6)
Cu(2)–Cl(2)	2.255(3)	Cu(2)–N(6)	2.321(7)
O(1)–Cu(1)–N(2)	164.2(3)	O(1)–Cu(1)–N(1)	83.4(3)
N(2)–Cu(1)–N(1)	86.1(3)	O(1)–Cu(1)–Cl(1)	90.9(2)
N(2)–Cu(1)–Cl(1)	95.9(2)	N(1)–Cu(1)–Cl(1)	163.0(2)
O(1)–Cu(1)–N(3)	103.4(3)	N(2)–Cu(1)–N(3)	87.3(3)
N(1)–Cu(1)–N(3)	85.0(3)	Cl(1)–Cu(1)–N(3)	111.9(2)
O(1)–Cu(2)–N(5)	163.8(3)	O(1)–Cu(2)–N(4)	83.6(3)
N(5)–Cu(2)–N(4)	87.6(3)	O(1)–Cu(2)–Cl(2)	90.0(2)
N(5)–Cu(2)–Cl(2)	95.2(2)	N(4)–Cu(2)–Cl(2)	165.2(2)
O(1)–Cu(2)–N(6)	107.0(3)	N(5)–Cu(2)–N(6)	85.5(3)
N(4)–Cu(2)–N(6)	83.8(3)	Cl(2)–Cu(2)–N(6)	110.9(2)
Cu(2)–O(1)–Cu(1)	115.1(3)		

Table 2 Selected interatomic distances (Å) and angles (°) for complex **4**

Cu(1)–O(1)	1.905(9)	Cu(1)–N(2)	2.028(9)
Cu(1)–N(1)	2.058(9)	Cu(1)–N(3)	2.261(9)
Cu(1)–Br(1)	2.392(2)	Cu(2)–O(1)	1.923(10)
Cu(2)–N(5)	2.019(10)	Cu(2)–N(4)	2.066(9)
Cu(2)–N(6)	2.334(9)	Cu(2)–Br(2)	2.405(2)
O(1)–Cu(1)–N(2)	163.5(4)	O(1)–Cu(1)–N(1)	82.5(4)
N(2)–Cu(1)–N(1)	86.4(4)	O(1)–Cu(1)–N(3)	104.1(4)
N(2)–Cu(1)–N(3)	87.1(4)	N(1)–Cu(1)–N(3)	85.6(4)
O(1)–Cu(1)–Br(1)	90.2(3)	N(2)–Cu(1)–Br(1)	96.6(3)
N(1)–Cu(1)–Br(1)	161.6(3)	N(3)–Cu(1)–Br(1)	112.7(3)
O(1)–Cu(2)–N(5)	161.5(5)	O(1)–Cu(2)–N(4)	83.0(4)
N(5)–Cu(2)–N(4)	86.8(5)	O(1)–Cu(2)–N(6)	107.7(4)
N(5)–Cu(2)–N(6)	86.1(4)	N(4)–Cu(2)–N(6)	82.8(4)
O(1)–Cu(2)–Br(2)	89.7(3)	N(5)–Cu(2)–Br(2)	96.7(3)
N(4)–Cu(2)–Br(2)	165.3(3)	N(6)–Cu(2)–Br(2)	111.6(3)
Cu(1)–O(1)–Cu(2)	116.2(5)		

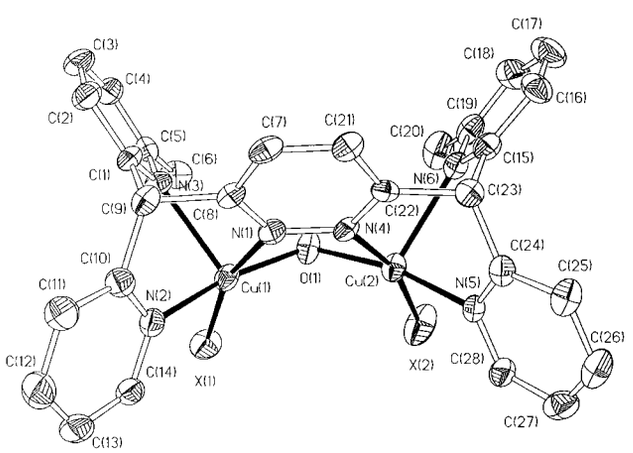

Fig. 4 A computer generated drawing of $[Cu_2(mbdpdz)X_2(OH)]X$ (X = Cl **3** or Br **4**)

For **3** Cu(1) lies 0.27 Å above the mean plane defined by the basal Cl(1)–O(1)–N(1)–N(2) [−0.036, 0.043, −0.046, 0.039 Å] atoms, while Cu(2) lies 0.26 Å above the equivalent mean plane defined by Cl(2)–O(1)–N(4)–N(5) [−0.005, 0.006, −0.007, 0.006 Å] atoms. The dihedral angle between these two planes is 64.6°. For **4** Cu(1) lies 0.29 Å above the mean plane defined by the basal atoms Br(1)–O(1)–N(1)–N(2) [−0.43, 0.055, −0.058, 0.046 Å], while Cu(2) lies 0.27 Å above the mean plane defined by atoms Br(2)–O(1)–N(4)–N(5) [0.009, −0.01, 0.01, −0.009 Å]. The dihedral angle between these two planes is 65.7°. The distortion from square-pyramidal geometry is greater for Cu(1) in both complexes.

Table 3 Internal coordinates of the hydrogen atom in the hydroxo ligand (complex **3** represented by X = Cl, complex **4** by X = Br), as optimized by molecular mechanics (MM+)

	Complex **3** (X = Cl)	Complex **4** (X = Br)
O–H bond length/Å	1.01	1.00
Cu(1)–O–H angle/°	110.4	104.6
Cu(2)–O–H angle/°	115.4	104.7
H–X(1)/Å	2.64	2.79
H–X(2)/Å	2.77	2.86

The copper–copper distance is identical in both complexes [3.251(2) Å], while the Cu(1)–O(1)–Cu(2) angles are 115.1(3) and 116.2(5)° for **3** and **4** respectively. This difference in the bridging angle modifies the Cu(1)–O(1) distance which is longer for complex **3** [Cu(1)–O(1) 1.930(7) Å] than for complex **4** [Cu(1)–O(1) 1.905(9) Å]. The Cu(2)–O(1) bond remains almost constant [1.921(6) and 1.923(10) Å for **3** and **4** respectively]. A similar interplay of the bridge angle with the Cu–O bond lengths has been reported by Thompson and co-workers.[9]

Although a hydrogen atom could not be located on O(1), other data, including an infrared absorption at 3540 cm^{-1} leave little doubt as to the identity of this bridging group as hydroxide.

The position of the hydroxo ligand hydrogen atom of complexes **3** and **4**, which X-ray diffraction could not yield, was refined with molecular mechanics. For molecular mechanics, the MM + force-field parameter set was slightly modified in order to account for the copper atom. The van der Waals parameters for Cu^{II} have been tested elsewhere with several types of ligands.[14,15] In order to take into account Cu–H 1,3-van der Waals and 1,3-electrostatic interactions, which revealed themselves as the most important, and which are used in inorganic molecular mechanics,[16] dummy C sp atoms were added at the middle of the Cu–O bond. As the MM+ force field only takes into account 1,4 non-bonded interactions, these C atoms served to make the 1,3 Cu–H interactions appear as 1,4 interactions to the force field, without modifying anything else in the calculation. Thus van der Waals and electrostatic Cu–H interactions could be taken into account, and the indeterminate Cu–O–H bending term could be bypassed, being transformed into C–O–H bending. Also, because of the uncertainty of the hydroxo-oxygen status in the complex, two atom types were tried for oxygen, O2 which corresponds to a sp^3 oxygen, and Of, the furan type, where the hybridization state is sp^2. Finally, only the former was retained since the two types gave results corresponding to a tetrahedral oxygen.

For both complexes **3** and **4**, the geometry optimization, performed without any constraint on the Cu–O–H angles, yielded a hydrogen atom with a Cu–O–H angle closer to 109° (tetrahedral) than to 122° (trigonal). The H · · · X distance from the geometry optimization also indicates a slight interaction (Table 3). In order to verify the possibility of existence of multiple minima, a graph of the strain energy *versus* the Cu–O–H angles (both set to the same values) is presented in Fig. 5. The 122° angle corresponds to a planar structure. Both Cu–O–H angles were then lowered towards to a tetrahedral structure with the constraint of both Cu–O–H angles being set to the same value (recorded on the *x* axis). The only minimum encountered lies above the Cu–O–Cu plane, obviously corresponding to an attractive interaction between H and Br.

Room-temperature magnetic moments per copper atom for complex **3** (μ_{eff} = 1.05 μ_B) and for complex **4** (μ_{eff} = 1.28 μ_B) indicate antiferromagnetic coupling between the copper(II) centres (Figs. 1 and 6). The polycrystalline EPR spectra of compounds **3** and **4** where recorded at X-band frequency at 300 K. The spectra have low absorption intensities and are poorly resolved in the $m_s = \pm 1$ region near $g = 2.1$, and no $m_s = \pm 2$ absorption was observed (Fig. 2). Probably the zero-field splitting tensor *D*

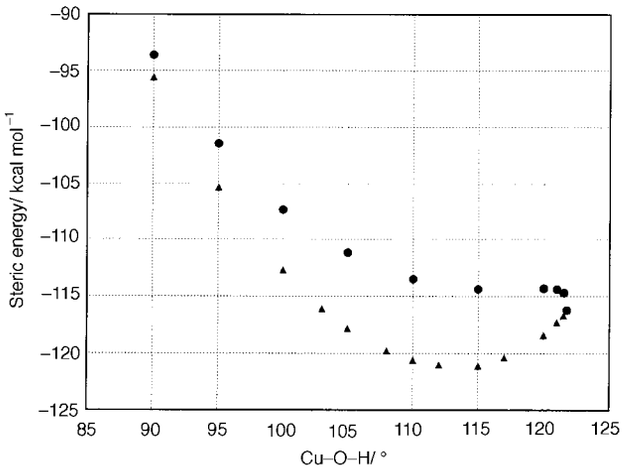

Fig. 5 A plot of MM+ steric energy *versus* Cu–O–H angle for complex **4**. Triangles correspond to the space portion located above the Cu–O–Cu plane where the bromine atoms lie, and circles to the other side of the plane

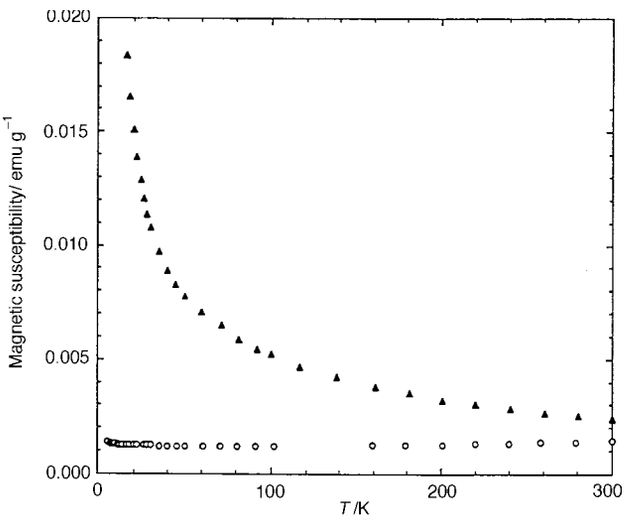

Fig. 6 Corrected magnetic susceptibility *vs.* temperature for (▲) $[Cu_2(mbdpdz)Br_4]\cdot H_2O$ **2** and (○) $[Cu_2(mbdpdz)Br_2(OH)]Br$ **4**

and the *g* tensor are not coaxial, so their principal values cannot be deduced from powder data as previously reported for highly coupled dicopper complexes.[17]

In contrast to the results for the chloro complex **1** and the bromo complex **2**, a much larger antiferromagnetic interaction is operating in complexes **3** and **4**. Since the differences in the ligands of complexes **1** and **3**, and **2** and **4** is obviously the presence of the hydroxide-oxygen which bridges the copper centres, the increase of the antiferromagnetic interaction should be caused by the hydroxo group. The dichloro and dibromo complexes **1** and **2** have metal centres which are probably bridged by an equatorial and an axial halogen ligand. Although halogen bridges are known to be superexchange active, the orientation of the magnetic orbitals of the metal centres in these complexes is such that effectively no antiferromagnetic exchange should be expected to occur *via* these bridging groups.[12] Therefore the diazene bridge is the only effective path for the magnetic interaction. As previously reported, when the two copper(II) ions are bridged by an extended ligand, the ferromagnetic component is actually very small and only the antiferromagnetic contribution is significant.[18,19]

In compounds **3** and **4** a slightly distorted pyramidal geometry of the Cu^{II} ions results in a ground state configuration of the complex dominated by $d_{x^2-y^2}$ orbitals that orient their lobes toward both the hydroxo- and pyridazine-bridging ligands. When the two copper(II) ions are bridged by an extended ligand such as pyridazine each magnetic orbital is delocalized over a large number of bridge atoms, consequently the overlap density is spread over the entire bridge. Both the σ and π orbitals of the pyridazine heterocycle should be capable of acting as superexchange pathways between copper(II) ions. The overlap of the copper magnetic orbitals and the σ and π orbitals of the nitrogen-containing heterocycles is maximum in a planar arrangement when the Cu–N–N angle is close to 120°. The values reported for the present pyridazine compounds **3** and **4** could explain partially the strong antiferromagnetic interaction [Cu(1)–N(1)–N(4) 117.6(5) and Cu(2)–N(4)–N(1) 117.5(6)°] for **3** and [Cu(1)–N(1)–N(4) 118.2(8) and Cu(2)–N(4)–N(1) 117.0(9)°] **4**. When the corresponding angle deviates significantly from the ideal value, as observed for triazole[2,20] and indazole[21,22] the exchange decreases. Besides, the moderately large Cu–O–Cu angles [115.1(3) and 116.2(5)° for **3** and **4** respectively] should result in good overlap between the copper $d_{x^2-y^2}$ orbital and the s and p orbitals of the oxygen atom, thus permitting the exchange interaction evidenced by the subnormal effective magnetic moments at room temperature.

In order to get a better insight into the above mentioned electronic effects, we have performed extended-Hückel[23] (EH) calculations on these compounds, with the use of the CACAO package.[24] The standard atomic parameters were used for C, O, N and H;[23,24] those of Cu, Cl and Br were taken from the literature.[25–27] Calculations were made on the experimental X-ray molecular structures, which are in both cases not far from the ideal C_s symmetry. The position of the hydroxo hydrogen atoms, not experimentally determined, were taken from force field-type calculations described above. The optimized Cu(1)–O–H and Cu(2)–O–H bond angles and O–H bond distance of **3** and **4** are given in Table 3. They clearly indicate a non-planar co-ordination (sp^3) of oxygen. This result is consistent with the absence of a vacant p-type orbital on any of the oxygen neighbours, which would allow conjugation. However, we were aware that the hybridization of oxygen could somewhat influence the energy and shape of the magnetic orbitals of **3** and **4**. This point has been discussed by others in the case of related compounds.[28–30] It turns out that the nature and energy of the magnetic orbitals are only very slightly dependent on the hybridization of oxygen, as experienced by EH calculations in which the Cu–O–H bond angles were varied from 100 to 120°. Therefore, the results described below correspond to the calculations made with the MM+ optimized hydrogen positions, which are likely to be close to the real ones.

As expected, **3** and **4** having very similar structures, lead to very similar results. In both compounds, the Cu···Cu overlap population is close to zero (−0.007 and −0.008 in **3** and **4**, respectively), indicating no direct through-space coupling between the metals. In agreement with the observed bond distances, the apical Cu–N overlap populations are much smaller than the equatorial ones. The corresponding averaged values for **3** are +0.150 and +0.299, respectively. In **4**, they are +0.151 and +0.300, respectively. The two magnetic orbitals of **3** are plotted in Fig. 7. Both are metal–ligand antibonding and have a large $d_{x^2-y^2}$ character, with no participation from the apical nitrogen atoms. This is in agreement with the pyramidal square-planar co-ordination mode of the metal atoms in **3** and **4**. In **3**, these two levels are separated by a gap of 0.20 eV. In the case of **4** it is 0.24 eV. The width of this gap varies as the square root of the antiferromagnetic coupling constant.[25] The magnetic orbital of lowest energy (φ_s) is the in-phase combination of the copper atomic orbitals (AO's), while the highest (φ_a) is the out-of-phase combination. As pointed out by others,[28,30–33] these orbitals mix in an antibonding way with AO's of the bridging oxygen atom. The φ_s orbital mixes with a s-type oxygen hybrid and φ_a mixes with the 2p(O) orbital which lies parallel to the Cu···Cu vector. As expected from the rather

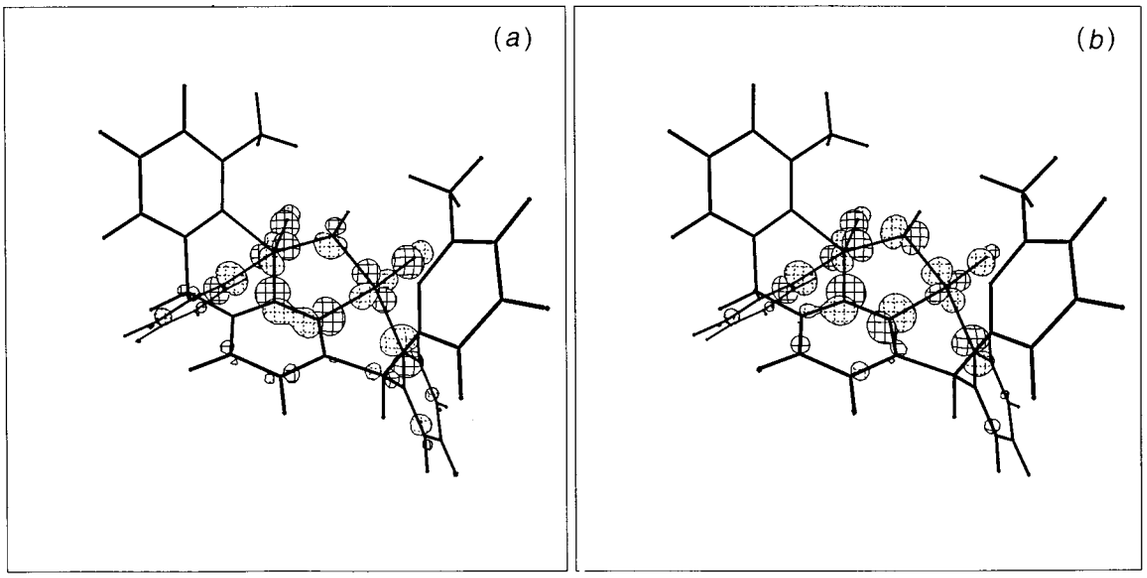

Fig. 7 Phase and spatial distribution of (*a*) symmetric φ_s and (*b*) antisymmetric φ_a magnetic orbitals

large Cu–O–Cu angle,[25] the Cu–O antibonding character is larger in φ_a than in φ_s. In the case of **3**, the average Cu–O overlap populations in φ_a and φ_s are −0.074 and −0.032 respectively; the corresponding values of **4** are −0.068 and −0.027.

As predicted by Nishida and Kida,[30] φ_s mixes in an antibonding way with an in-phase combination of s-type diazenic nitrogen hybrid AO's, while φ_a mixes in an antibonding way with the out-of-phase combination of the same hybrids. As a consequence, φ_s presents some N–N bonding character, as exemplified by its N–N overlap population which is +0.040 in **3** and +0.038 in **4**. On the other hand, φ_a is N–N antibonding with a corresponding overlap population of −0.061 in **3** and −0.068 in **4**.

Therefore, at least two important geometrical parameters are responsible for the existence of a gap between φ_s and φ_a, and consequently for the antiferromagnetic behaviour of **3** and **4**. One is the large Cu–O–Cu angle which renders φ_a more Cu–O antibonding than φ_s. The second one is the rather short N–N separation which renders φ_a significantly N–N antibonding and renders φ_s N–N bonding. One should however be aware that other factors are contributing to the energies of φ_s and φ_a. In particular, these two orbitals differ also significantly by their Cu–N (diazene) character; φ_s is more Cu–N antibonding than φ_a. In **3**, the corresponding average overlap populations in these two levels are −0.055 and −0.026, respectively; in **4**, they are −0.050 and −0.023. The origin of this difference, which tends to lower the gap between φ_s and φ_a, is difficult to rationalize simply. A careful analysis of the wavefunction indicates that the other ligands (*i.e.* the halogen and the equatorial pyridinic ring) play some role in the difference of Cu–N (diazene) antibonding character of φ_s and φ_a. Another crucial geometric factor is the degree of planarity of the CuNNCu sequence. In **3** and **4** the CuNNCu torsional angle is close to zero (3.2 and 2.7°, respectively). In this situation, the nitrogen σ-type hybrids which participate in φ_s and φ_a have their overlap close to maximum, contributing largely to the existence of a gap between the magnetic levels. This is not the case, for instance in similar compounds $[Cu_2(bdpdz)Cl_3(H_2O)]Cl$ and $[Cu_2(bdpdz)Br_4]$ in which this torsional angle is much larger (18.2 and 16.6°, respectively), and is reflected in low antiferromagnetic interactions.[12] This may be part of the reason why **1** and **2**, assuming similar structures to the above mentioned compounds, are less magnetically coupled than **3** and **4**. The position of the oxygen atom with respect to the mean plane of the ring is also important. If it was closer to the plane, stronger Cu–O interactions would result, leading to a larger difference in the Cu–O antibonding character of φ_s and φ_a.

Finally, it should be noted that the various structural parameters described above are not independent, due to the strain in the CuNNCuO ring. Changing one of them would result in changing them all. As a consequence, it is not really possible to identify a single parameter which would be the only significant factor affecting the magnetic exchange in **3** and **4**.

Experimental

Syntheses

(6-Methyl-2-pyridyl)(2-pyridyl)methane was prepared by a literature method.[34]

3,6-Bis[(6-methyl-2-pyridyl)(2-pyridyl)methyl]pyridazine (mbdpdz). This compound was prepared by addition of 3,6-dichloropyridazine dissolved in diethyl ether to a solution of (6-methyl-2-pyridyl)(2-pyridyl)methyllithium in the same solvent at −20 °C. The reaction mixture was allowed to reach room temperature, and then water was added to destroy any unreacted organolithium compound. The insoluble solid was filtered off, washed with water and vacuum dried; yield 40%. ^{1}H NMR ($CDCl_3$): δ 2 (s, 6 H, methyl protons), 6 (s, 2 H, methyne protons), 6–7 (m, 14 H, aromatic protons) and 8.5 (dd, 2 H, pyridine α protons).

$[Cu_2(mbdpdz)Cl_4]$ 1 and $[Cu_2(mbdpdz)Br_4]$ 2. A solution of mbdpdz (1 mmol) in methanol (15 cm^3) was added to a warm solution (5 cm^3) of $CuBr_2$ or $CuCl_2{\cdot}2H_2O$ (3 mmol) in the same solvent. The green precipitate obtained was insoluble in most common solvents and was used without further purification. Elemental analysis (C, H, N) were performed by the microanalytical service of CEPEDEQ of the Universidad de Chile {Found for **1**: C, 43.7; H, 3.7; Cl, 17.8; Cu, 16.45; N, 10.9. Calc. for $[Cu_2(mbdpdz)Cl_4]{\cdot}2H_2O$: C, 44.86; H, 3.74; Cl, 18.96; Cu, 16.96; N, 11.21%. Found for **2**: C, 37.0; H, 2.8; Br, 33.4; Cu, 13.5; N, 9.2. Calc. for $[Cu_2(mbdpdz)Br_4]{\cdot}H_2O$: C, 36.96; H, 2.86; Br, 35.2; Cu, 13.98; N, 9.24%}.

$[Cu_2(mbdpdz)Cl_2(OH)]Cl$ 3 and $[Cu_2(mbdpdz)Br_2(OH)]Br$ 4. Aqueous acetonitrile suspensions of **1** and **2** were refluxed until the solid dissolved completely. The solutions were left for several days; on standing blue crystals of **3** and **4** suitable for X-ray diffraction studies separated {Found for **3**: C, 47.9; H, 3.6; Cl, 14.9; Cu, 18.3; N, 11.9. Calc. for $[Cu_2(mbdpdz)Cl_2(OH)]Cl$:

Table 4 Crystallographic data and refinement details for complexes **3** and **4**

Formula	$C_{28}H_{25}Cl_3Cu_2N_6O$	$C_{28}H_{25}Br_3Cu_2N_6O$
M	694.97	828.35
Crystal system	Monoclinic	Monoclinic
Space group, number	$C2/c$ (no. 15)	$C2/c$ (no. 15)
Crystal size/mm	0.30 × 0.20 × 0.16	0.18 × 0.12 × 0.09
Crystal colour, habit	Prismatic, light blue	Prismatic, dark blue
a/Å	28.364(3)	28.528(5)
b/Å	13.511(1)	13.459(2)
c/Å	16.858(1)	17.348(3)
β/°	109.70(1)	109.35(1)
U/Å^3	6082.3(9)	6284.8(18)
Z	8	8
D_c/g cm^{-3}	1.52	1.75
F(000)	2816	3248
μ/mm^{-1}	1.69	5.20
θ Range/°	1.69–22.55	1.51–22.55
Index ranges	$-30 \leqslant h \leqslant 29$, $0 \leqslant k \leqslant 14$, $-1 \leqslant l \leqslant 18$	$-30 \leqslant h \leqslant 28$, $0 \leqslant k \leqslant 14$, $0 \leqslant l \leqslant 18$
Collected reflections	4484	5796
Independent reflections (R_{int})	4003 (0.033)	4084 (0.040)
Observed reflections [$F^2 > 2\sigma(F^2)$]	2501	2202
Absorption correction	None	None
$R1$, $wR2$ [$F^2 > 2\sigma(F^2)$]	0.069, 0.204	0.085, 0.217
$R1$, $wR2$ (all data)	0.108, 0.226	0.151, 0.264

C, 48.35; H, 3.63; Cl, 15.30; Cu, 18.26; N, 12.09%. Found for **4**: C, 40.1; H, 3.0; Br, 28.0; Cu, 15.3; N, 10.0. Calc. for [Cu_2(mbdpdz)Br_2(OH)]Br: C, 40.56; H, 3.02; Br, 28.97; Cu, 15.32; N, 10.14%}.

X-Ray crystallography

Crystal data, data collection and processing; structure analysis and refinement for complexes **3** and **4** are summarized in Table 4.

Crystallographic programs employed were the Siemens data collection software and SHELXTL PLUS.[35] Scattering factors were from ref. 36.

Both complexes are stabilized by an external, non-co-ordinated halogen atom. The latter is found to be severely disordered into a number of partially occupied sites. The occupancies of the halogen atom were restrained during refinement to add to one, in accordance to the known chemical composition. As a result of this severe disorder, the diffraction data were of a rather poor quality, and although good enough to allow a reasonable model to be found by Patterson methods, it prevented any successful unassisted refinement of the latter. The problem could only be circumvented by imposing a set of similarity restraints to homologous distances in the structures. With these set of metric restrictions in force, refinement on F^2 converged rather smoothly to the final values reported in Table 4.

CCDC reference number 186/690.

Magnetic measurements

Samples were used as powders for magnetic susceptibility measurements. Magnetic susceptibility data were obtained between 5 and 300 K using a SHE 906 SQUID magnetometer, at a field of 1 kOe (10^3 A m^{-1}). For complex **2** magnetic measurements were repeated at the low-temperature range from 2.24 to 7.03 K in order to minimize the experimental error.

Pascal's constants were used to estimate the correction of diamagnetism of the sample, and the temperature–independent paramagnetism contribution for each copper atom was taken as 60 cm^3 mol^{-1}.

Molecular mechanics

In order to refine the position of the hydroxo ligand hydrogen atom which X-ray diffraction could not yield, in complexes **3** and **4**, a molecular mechanics analysis was performed. The software package HYPERCHEM 4.5 was used.[37]

The MM+ force field was used, along with the introduction of one new atom type for copper and corresponding van der Waals parameters.[14] As no dipole moments involving Cu were available, the electrostatic term was chosen as point charges, with the charges calculated using the extended-Hückel method. All atoms were frozen in their crystallographic positions except for the hydrogen, and geometry optimization was performed, using the block-diagonal Newton–Raphson optimizer, with a root mean square limit of 0.01 kcal mol^{-1} Å^{-1} for the gradient. For the potential energy graph, single point energies were calculated with the additional constraint of both Cu–O–H angles being fixed at the same value, the value used as the abscissa on the graph of Fig. 5.

Acknowledgements

This research was supported in part by the Fondo Nacional de Ciencia y Tecnología (Proyectos FONDECYT 1931001 and 1940515), and by Fundación Andes. We are also grateful to the Centre National de la Recherche Scientifique–Comisión Nacional de Investigacion Cientifica y Tecnologica collaboration program for financial support.

References

1 L. K. Thompson, V. T. Chacko, J. A. Elvidge, A. B. P. Lever and R. V. Parish, *Can. J. Chem.*, 1969, **47**, 4141.
2 J. C. Dewan and L. K. Thompson, *Can. J. Chem.*, 1982, **60**, 121.
3 D. V. Bautista, J. C. Dewan and L. K. Thompson, *Can. J. Chem.*, 1982, **60**, 2583.
4 L. K. Thompson, *Can. J. Chem.*, 1983, **61**, 579.
5 L. K. Thompson, F. W. Hartstock, P. Robichaud and A. W. Hanson, *Can. J. Chem.*, 1984, **62**, 2755.
6 L. K. Thompson, A. V. Hanson and B. S. Ramaswamy, *Inorg. Chem.*, 1984, **23**, 2459.
7 G. Bullock, F. W. Hartstock and L. K. Thompson, *Can. J. Chem.*, 1983, **61**, 57.
8 L. K. Thompson, T. C. Woon, D. B. Murphy, E. J. Gabe, F. L. Lee and Y. Le Page, *Inorg. Chem.*, 1985, **24**, 4719.
9 T. C. Woon, R. McDonald, S. K. Mandal, L. K. Thompson, S. P. Connors and A. W. Addison, *J. Chem. Soc.*, *Dalton Trans.*, 1986, 2381.
10 L. K. Thompson and T. C. Woon, *Inorg. Chim. Acta*, 1986, **111**, 45.
11 L. Rosenberg, L. K. Thompson, E. J. Gabe and F. L. Lee, *J. Chem. Soc.*, *Dalton Trans.*, 1986, 625.
12 J. Manzur, A. M. García, R. Letelier, E. Spodine, O. Peña, D. Grandjean, M. M. Olmstead and B. C. Noll, *J. Chem. Soc.*, *Dalton Trans.*, 1993, 905.
13 B. Bleaney and K. D. Bowers, *Proc. R. Soc. London*, *Ser. A*, 1952, **214**, 451.

14 K. R. Adam, M. Antolovich, D. Baldwin, P. Duckworth, A. Leong, L. Lindoy, M. McPartlin and P. Tasker, *J. Chem. Soc.*, *Dalton Trans.*, 1993, 1013.
15 M. Drew and P. Yates, *J. Chem. Soc.*, *Dalton Trans.*, 1987, 2563.
16 P. Bernhardt and P. Comba, *Inorg. Chem.*, 1992, **31**, 2638.
17 O. Kahn, T. Mallah, J. Gouteron, S. Jeannin and Y. Jeannin, *J. Chem. Soc.*, *Dalton Trans.*, 1989, 1117.
18 R. D. Willett, D. Gatteschi and O. Kahn, *NATO ASI Ser.*, *Ser. C*, 1985, **24**, 850.
19 O. Kahn, *Angew. Chem.*, *Int. Ed. Engl.*, 1985, **24**, 850.
20 A. Bencini, D. Gatteschi, C. Zanchini, J. G. Haasnoot, R. Prins and J. Reedijk, *Inorg. Chem.*, 1985, **24**, 2812.
21 G. Kolks and S. J. Lippard, *Acta Crystallogr.*, *Sect. C*, 1984, **40**, 261.
22 D. W. Phelps, W. F. Little and D. J. Hodgson, *Inorg. Chem.*, 1976, **15**, 2263.
23 R. Hoffmann, *J. Chem. Phys.*, 1963, **39**, 1397; R. Hoffmann and W. N. Lipscomb, *J. Chem. Phys.*, 1962, **36**, 2179; J. H. Ammeter, H.-B. Bürgi, J. C. Thiebault and R. Hoffmann, *J. Am. Chem. Soc.*, 1978, **100**, 3686.
24 C. Mealli and D. M. Proserpio, *J. Chem. Educ.*, 1990, **67**, 399.
25 P. J. Hay, J. C. Thiebault and R. Hoffmann, *J. Am. Chem. Soc.*, 1975, **97**, 4884.
26 R. H. Summerville and R. Hoffmann, *J. Am. Chem. Soc.*, 1976, **98**, 7240.
27 S. Alvarez, F. Mota and J. Novoa, *J. Am. Chem. Soc.*, 1987, **109**, 6586.
28 W. Mazurek, B. J. Kennedy, K. S. Murray, M. J. O'Connor, J. R. Rodgers, M. R. Snow, A. G. Wedd and P. R. Zwack, *Inorg. Chem.*, 1985, **24**, 3252.
29 M. Mikuriya, K. Toriumi, T. Ito and S. Kida, *Inorg. Chem.*, 1975, **24**, 3258.
30 Y. Nishida and S. Kida, *Inorg. Chem.*, 1988, **27**, 447.
31 Y. Nishida and S. Kida, *J. Chem. Soc.*, *Dalton Trans.*, 1986, 2633.
32 L. K. Thompson, S. K. Mandal, S. S. Tandon, J. N. Bridson and M. K. Park, *Inorg. Chem.*, 1996, **35**, 3117.
33 H. Nie, S. M. Aubin, M. S. Mashuta, R. A. Porter, J. F. Richardson, D. N. Hendrickson and R. M. Buchanan, *Inorg. Chem.*, 1996, **35**, 3325.
34 A. M. García, J. Manzur, E. Spodine, R. Baggio and M. T. Garland, *Acta Crystallogr.*, *Sect. C*, 1994, **50**, 1882.
35 G. M. Sheldrick, *SHELXTL PLUS*, *User's Manual*, Nicolet Instrument Co., Madison, WI, 1986.
36 *International Tables for X-Ray Crystallography*, Reidel, Boston, 1992, vol. C.
37 HYPERCHEM version 4.5, Hypercube Inc., Waterloo, Ontario, 1995.

Received 29*th May* 1997; *Paper* 7/03716C